Composite Structures 207 (2019) 909–922

Contents lists available at ScienceDirect

Composite Structures

journal homepage: www.elsevier.com/locate/compstruct

Optimal design of fighter aircraft wing panels laminates under multi-load case environment by ply-drop and ply-migrations

Sachin Shrivastava[a], P.M. Mohite[a,*], M.D. Limaye[b]

[a] Department of Aerospace Engineering, Indian Institute of Technology Kanpur, UP 208016, India
[b] R&D Engineers, DRDO, Pune, MH 411015, India

ARTICLE INFO

Keywords:
Ply-drop
Ply migration
Composite wing box design
Laminate blending
Multi-objective optimization
Python-scripting

ABSTRACT

The ply-drop (PD) is termination of specific plies at rib-axis for getting tapered laminates. The present optimization study aims to achieve minimum weight tapered wing panels laminates by PD followed by ply-migrations (PM). The PM are required for ply-continuity (blending) and achieving smooth external aerodynamic surface. A genetic-algorithm mutation operator and fitness based search algorithm is developed in the present study for the optimization. The laminate weight minimization has been achieved as goal of multi-objective optimization (MOO), by utilizing excess design margins of Tsai-Wu first ply failure-index (FI) and wing tip lateral deflection. The finite-element (FE) model of laminate is a set of discrete laminates (chromosomes) between ribs with continuity by virtue of ply-orientations. To select best fit laminate, ply orientations were randomly selected and perturbed for thickness during optimization. The fitness function for evaluating chromosomes is a composite function of multi-objective design requirements and design constraints. The algorithm submits orientation/thickness combinations to ABAQUS/CAE by python-script for function evaluation. The application of algorithm over an initially assumed quasi-isotropic laminate of uniform thickness showed 57% weight reduction for a fighter aircraft's wing panel. The optimization process is automated making PD practically viable in the design process itself.

1. Introduction

The aerospace structures like wing, fuselage, etc. are now coming up with high strength light weight fibrous composites with prepreg construction. Often such structures have tapering thickness laminates by virtue of experienced loads. The tapering of laminates have potential for significant weight reductions in engineering structures. Unlike metals, continuous tapering of laminates is not possible, therefore, plies are dropped at different locations to achieve tapering. The termination of plies at the rib-axis is termed as ply drop (PD). In the present study, an attempt has been made to design tapering wing panel laminates by optimally terminating uni-directional carbon fibre composite plies near the ribs as shown in Fig. 1. The PD is governed by a genetic-algorithm mutation operator and fitness based search algorithm followed by ply migrations (PM) for achieving blended and smooth external surface laminates. The smoothness of laminate top surface is an aerodynamic requirement to avoid separation of air-flow.

The literature review on weight minimization studies shows that many researchers have attempted re-orientation and deletion of plies in laminate by governing laminates through evolutionary algorithms. It is very well discussed that the re-orientation and deletion of plies in a laminate provide ample scope for laminate optimization [1–5]. However, very few researchers have worked on PD design aspect, which can further refine the optimization procedure to get significant amount of weight savings for the structure under design. Weigang et al. [6] attempted such an optimization for wing-box by proposing group of laminates with same ply-orientations, considering thickness and length of lamina groups as design variables for the design of blended laminates. Irisarri et al. [7] introduced stacking sequence (SS) tables to obtain optimal tapered laminates. They have optimized a 18-panel benchmark problem under buckling criterion with a set of guidelines, which were important from the aspect of de-lamination and manufacturing. Some of the guidelines like symmetry, balanced, covering and continuity from [7,8] were part of the present study. Liu et al. [9] minimized material volume of laminate for 18-panel benchmark problem for buckling and strain, by local level stack shuffling to satisfy blending [10] for manufacturability and proposed lamination parameter change to get optimal SS. Jin et al. [11] proposed an optimization framework on 18-panel problem under buckling by GA with least squares fitting to get fully blended optimal laminates. Adams et al. [12] optimized aircraft

* Corresponding author.
E-mail address: mohite@iitk.ac.in (P.M. Mohite).

https://doi.org/10.1016/j.compstruct.2018.09.004
Received 13 July 2018; Accepted 13 September 2018
Available online 20 September 2018

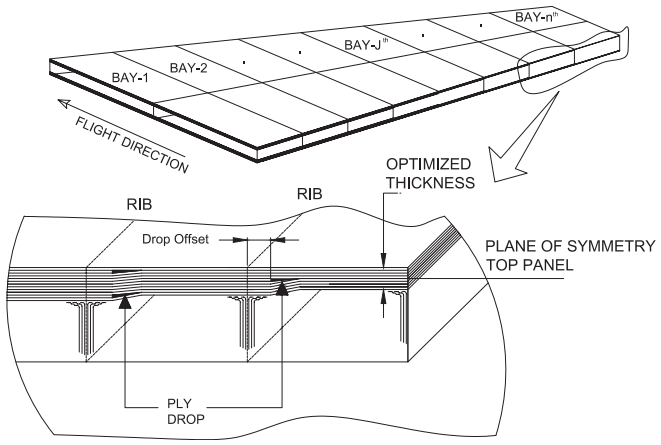

Fig. 1. Ply blending in wing box geometry.

laminated stiffened panels using GA for SS with objective function based on mismatch severity in adjacent laminates. The blending process of laminates was governed by the distance between population and set of lamina from adjacent population. Seresta et al. [13] optimized wing box (WB) by decomposing wing panel into independent local panels and attempted addition/deletion of plies while maintaining blending with adjacent panels. Daoust and Hoa [14] studied strength aspect with respect to internal/external and location of PD by extensive FE model. They have suggested that internal PD is almost twice strong compared to external PD. Rasul [15] carried out dynamic and stress analysis with development of an extensive finite element program over the variable thickness laminated composite beams. Their results suggest that the mid-plane PD leads to lower value of natural frequencies in dynamic analysis. However, the stress analysis suggests that discontinuities in terms of material and geometric at PD locations lead to significant change in stressing. Ganesan [16] determined the first-ply failure load, ultimate failure load, buckling load and maximum transverse displacements for different types of tapered laminated plates.

The weight optimization is often associated with reduction in margin of safety (MOS) over the design criteria. In general, the minimum positive MOS in strength, stiffness and buckling design criteria are necessary and sufficient requirements for design. The structures with positive MOS are safe in its operating conditions, where the operating conditions call for multiple design load cases. In engineering designs, higher MOS doesn't add value to the design, therefore, it is desirable that MOS for all the design criteria should get utilized towards the weight minimization while optimization. As these requirements are to be addressed simultaneously, therefore, the problem is treated as MOO problem, in which MOS (if available) must be utilized towards achieving minimum weight as a specific choice of weight vector w_i in the MOO. However, the literature review on design of tapered laminates shows that the optimizations attempted over laminated plates are based on single criterion. Therefore, there is need to explore MOO for the design of tapering laminates.

In the present study, an attempt has been made to design minimum weight WB panels laminates for a fighter aircraft. In WB, the wing bending moments become less severe as one move from root to tip. The reduction in load intensity promotes designer to use tapering sections for structural members, to achieve minimal laminate weight. The PD location is decided by optimization algorithm, which uses mutation operator and fitness based string selection of classical GA to drop the plies. The search algorithm drops the plies at rib-axis by converting thickness of plies from 0.15 mm to 0.001 mm [5] to achieve minimum laminate weight by compromising MOS within the limits, in multiple design load case. The present study further details the formation of chromosomes with lamina orientation and thickness information over discretized laminates (assumed) in ABAQUS Laminate Modeller (ALM). The information then flows in the form of well formed arrays in algorithm for the determination of PD followed by PM. The algorithm was defined in MATLAB and linked to ALM for function evaluation by a *python-script*. The selection of orientations of plies, which will participate to form laminate and their thickness perturbation (mutation) in subsequent iterations was based on random-number generator. The algorithm to search laminates of minimal weight under multi-objective design criterion is discussed by application of algorithm on a two load case (LC) problem.

2. Problem definition

The PD is an essential requirement for wing panel design to smoothly taper down thickness of top/bottom panel laminates from the root towards the tip. The smooth tapering can be achieved by ending plies in steps after drop-offset distance, as shown in Fig. 1. The drop-offset is required to avoid local stress concentrations and taken care during manufacturing. The present problem addresses the identification of location for termination of individual ply, based on value of fitness function, which is a combination of design requirements and laminate weight for different load cases. This is discussed in following section. The ply flow/drop design of tapering laminates (wing top/bottom panel) is based on a typical *design-rule*. The *design-rule* is stated as '*once a ply is dropped in a particular bay, it is not allowed to re-appear in subsequent bays and non-terminating plies have to be present in adjacent bays*'. This design rule is incorporated to chromosomes by alteration of thickness and ply-orientation variable by the algorithm discussed in Section 3.2. To decide PD in *n*th-bay, the algorithm tests the chromosomes formed by random mutation for fitness by submitting it to ABAQUS/CAE solver via *python-script*. The outcome of this study brings out dropping of plies near the rib-axis along with backward continuity.

2.1. Chromosome

The space between the adjacent wing-ribs is termed bay and a chromosome is mathematical representation of a bay-laminate. The representation of a chromosome in the present study is based on two arrays. These arrays are $[T]$ and $[PLYOR]$, where $[T]$ has information about thickness (existence) of a ply while $[PLYOR]$ has information about ply-orientation of *i*th ply in *j*th bay. These two arrays have master-slave arrangement such that any change to $[T]$ is reflected on $[PLYOR]$ and they must be read in conjunction. This section gives a sample formation of top panel laminate of size as shown in Fig. 2, which has 3 symmetric plies running through the 4 bays. The laminate in Fig. 2a is an initial laminate of uniform thickness having ply-flow through all the bays. However, Fig. 2b shows ply-termination at specific ribs in terms of $[T]$, where $T_{ij} = 1 / 0$ corresponds to 0.15 mm/0.001 mm thickness [5]. The 0.001 mm ply thickness corresponds to non-existence of the ply in laminate. The initial laminate has been redesigned to form the laminate shown in Fig. 2b after PD. The equivalent array representation considering symmetry for the two cases of Fig. 2 is given as,

$$[T] = \begin{bmatrix} 1 & 1 & 1 & 1 \\ 1 & 1 & 1 & 1 \\ 1 & 1 & 1 & 1 \end{bmatrix} \quad \text{and} \quad [PLYOR] = \begin{bmatrix} 0 & 0 & 0 & 0 \\ 45 & 45 & 45 & 45 \\ 90 & 90 & 90 & 90 \end{bmatrix} \tag{1}$$

after PD and PM,

$$[T] = \begin{bmatrix} 1 & 1 & 1 & 1 \\ 1 & 1 & 0 & 0 \\ 1 & 0 & 0 & 0 \end{bmatrix} \quad \text{and} \quad [PLYOR] = \begin{bmatrix} 0 & 0 & 0 & 0 \\ 45 & 90 & . & . \\ 90 & . & . & . \end{bmatrix} \tag{2}$$

The array obtained can be altered by algorithm during optimization. The ply-flow after optimization is updated by virtue of *ply-migration*. The ply flow after PM can be seen by $[PLYOR]$. In PM, as a ply is dropped, ply below the dropped-layer shifts upward to take the position of dropped ply in the subsequent bay as shown in Fig. 2b. The ply

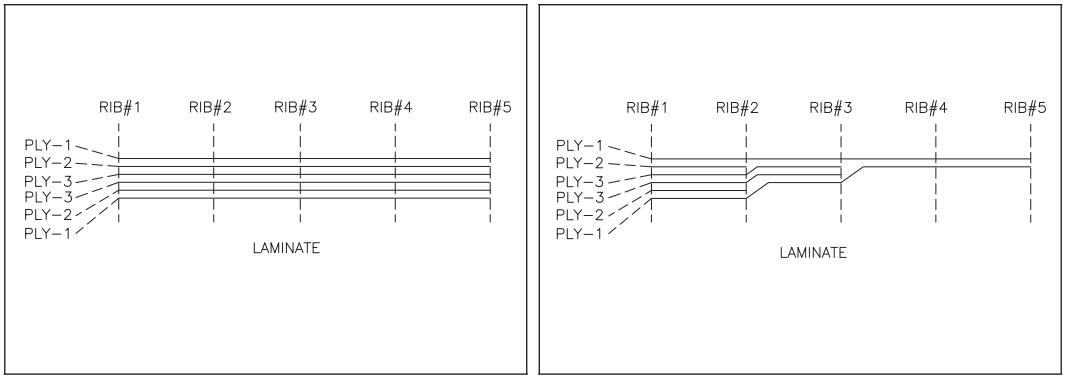

Fig. 2. PD and PM in [6 × 4] laminate with ply-1(0^0), ply-2(45^0), ply-3(90^0). (a) Starting laminate (b) Final Laminate.

arrangement can be treated as discrete laminates in different bays, however, the continuity of plies is by virtue of ply-orientations in subsequent bays that are being translated to FE model.

2.2. Problem size

Each ply in a laminate can have two possibilities, $T_{ij} = 1\text{or}0$. Therefore, the possible independent arrangements of Fig. 2 ($i \times j$ size) laminate considering symmetry is 2^{i*j}. However, the SS in bays are interconnected and mismatches in their orientations and thicknesses are not allowed [7]. Therefore, the number of possible arrangements reduces to $2^{i}*j$. During kth bay iteration, ply variables are copied from kth-bay to subsequent bays. Thus, the kth-bay SS becomes the guiding SS for subsequent bays. Apart from that, as discussed above the thickness array (master) is followed by ply-orientation array (slave) to maintain ply arrangement during PM. The master-slave arrangement is a part of optimization algorithm. Thus, the additional information about the ply-orientation associated with each laminate does not increase the problem size.

2.3. Design criteria

The limiting values of Tsai-Wu failure index (*FI*), buckling eigenvalue λ (see Fig. 2) and lateral deflection δ (see Fig. 3b) were design criteria for the present study. The Tsai-Wu failure index (*FI*) was based on Tsai-Wu [17] first-ply failure theory as,

$$FI = \sigma_1\left(\frac{1}{X_t}-\frac{1}{X_c}\right)+\sigma_2\left(\frac{1}{Y_t}-\frac{1}{Y_c}\right)-\frac{\sigma_1^2}{X_t*X_c}-\frac{\sigma_2^2}{Y_t*Y_c}-\frac{\sigma_{12}^2}{S^2} \tag{3}$$

where, X, Y are lamina strengths in x-direction and y-direction, S is shear strength in xy-direction, respectively. The subscripts t and c denote tensile and compressive nature, respectively [18].

The *FI* criterion gives estimation of static strength of the laminated structure. However, the lateral deflection δ suffices for the stiffness requirement and λ as a measure of buckling reserve factor [19] of the structure under different load conditions. For the optimal design, MOS for static strength, lateral deflection has to be a minimum positive value. However, the buckling eigenvalue must be greater than one to have the structure, which is free from buckling.

2.4. Fitness function

The changes in thickness and ply-orientations change the fitness of chromosome, which is the basis of its selection in next generation. The fitness function Z given by Eq. (4), is a combination of laminate weight minimization along with minimization of MOS for FI and lateral deflection. The fitness function is designed based on penalty approach [20,21], in which double-sided penalty will be imposed, subject to deviation of design criterion from its allowable value, therefore, the function Z does not remain minimal. The study attempts simultaneous minimization of MOS in different design criteria to get a weight minimized structure. Therefore, the optimization problem in mathematical form is written as;

$$\begin{aligned} Minimize\, f_1(FI) &= (1.0-FI)*s_{fi} \quad \text{when } FI \leqslant 1.0 \\ &= LN \quad \text{when } FI > 1.0 \\ Minimize\, f_2(\delta) &= (\delta_a-\delta)*s_{def} \quad \text{when } \delta \leqslant \delta_a \\ &= LN \quad \text{when } \delta > \delta_a \\ Minimize\, f_3 &= L_w*s_{lw} \\ Subject\ to \lambda &\geqslant 1 \end{aligned}$$

The fitness function/composite function with weight vector $(w_1, w_2, w_3)^T$ formed as:

$$Minimize\ Z = w_1*f_1 + w_2*f_2 + w_3*f_3 \tag{4}$$

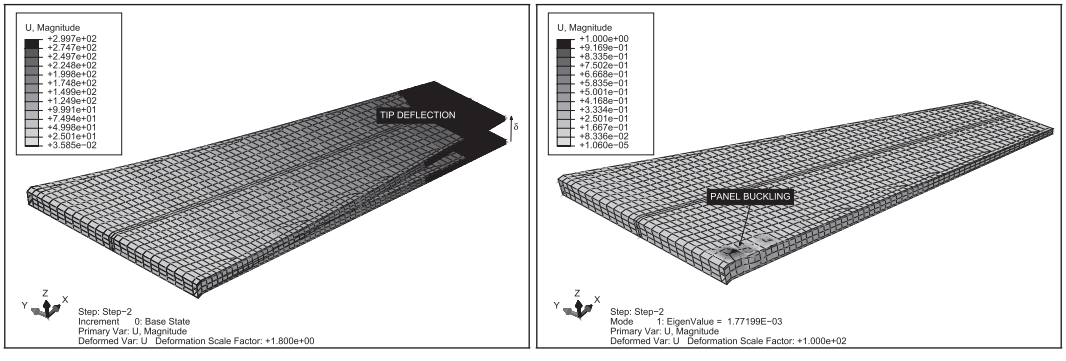

Fig. 3. Design criteria (a) Wing lateral deflection (δ) (b) Eigenvalue of Panel buckling (λ).

where, *FI* is Tsai-Wu first ply FI, δ is wing lateral deflection, δ_a maximum allowed wing lateral deflection, λ is buckling eigenvalue, L_w is the laminate weight, *LN large-number* and s_{fi}, s_{def} and s_{lw} are scaling factors and w_i are the weights over *FI*, δ and L_w, respectively.

The penalty functions $f_1(FI)$ and $f_2(\delta)$ correspond to static strength penalty and lateral deflection penalty. When *FI* or δ value is deviated from its design allowable, the $f_1(FI)$, $f_2(\delta)$ impose penalty on the fitness function *Z*. The penalty will be of smaller magnitude if design criteria are within design allowables, however it will be a *large-number* if design criteria exceed design allowables.

The different design criteria have different working ranges during optimization. Therefore, the objective functions must be normalized (scaled) before its use in fitness function. The scaling factors $s(x_i)$ associated to Eq. (4) [22] can be evaluated based on one of the design variable (x_c) as

$$s(x_i) = \frac{max.(x_i) - min.(x_i)}{max.(x_c) - min.(x_c)} \tag{5}$$

The weights w_i in Eq. (4) prioritize the importance of design variables during optimization. The weights w_i were fractions with $\sum_{i=1}^{N} w_i = 1$, where *N* is the number of objective functions. The weight vector selection and scaling factor estimation are discussed in Section 5.1.

2.5. Random mutation: Transformation to dummy plies

The mutation operator of the classical GA using MATLAB random number generator is developed here to form a random-mutation operator for designing the present PD algorithm. The random-mutation is conversion of real ply to dummy ply by changing thickness parameter, which is showed by [*PLYOR*] array of representative chromosome of Fig. 4. The Fig. 4a shows 4th-bay string being subjected to random-mutation, in which $T_{2,4}$ and $T_{7,4}$ are randomly selected laminae and their thicknesses are changed from 0.15 mm to 0.001 mm. The removal of layer(s) in FE model is incorporated by conversion of real-ply to dummy-ply by changing thickness from 0.15 mm to 0.001 mm. This change is represented on [*PLYOR*] as shown in Fig. 4b. The information of 4th-bay is then copied to subsequent bays to obey the *design-rule* discussed in Section 2. Briefly, a random-mutation is an operator, which perturbs randomly selected bits of *i*th-bay to convert real ply to dummy ply followed by copying of the information over the subsequent bays. The Fig. 5 shows action of random-mutation operator on the chromosome by [*T*]. The Fig. 5 shows random-mutation possibilities and select one of the mutation-possibility to update information of the entire chromosome based upon its fitness value.

3. Submission of FE problem to solver

The lamination of the tapered wing panels is defined in ALM. The ALM assigns ply-thickness and orientations to specified regions of the shell elements, which correspond to the bays of wing geometry. By defining separate laminate for each bay (discretization) in ALM, one can govern entire lamination with [*T*] and [*PLYOR*] as in Eqs. (1) and (2), respectively. The lamination parameters of ALM are updated and submitted to FE solver by MATLAB through *python-scripting*, which is linked to MATLAB based algorithm. The algorithm for the determination of PD location has to cater for two aspects; first, which orientation ply has to be dropped and second, where it is to be dropped. To address the issue, algorithm alters the ALM by random mutations.

3.1. Python script

The algorithm generates sets of variables during optimization for which the FE problem needs to be evaluated. The *python-script* works as an interface between the FE model and algorithm generated parameters. The Table 1 shows *python-script*, which is the part of the present optimization algorithm. The script solves the FE problem for MATLAB generated parameters for a *k*th load case. The *python-script* reads variables generated by MATLAB (line number 2). The line number 4 assigns parameters to ALM. Then the line numbers 6 and 15 submit the model for FE static and buckling analyses, respectively. At the end of static and buckling solutions, the result files are written (line numbers 11 and 16). The result files were read by MATLAB to guide the algorithm for its further generations. The script line number 4 is repeated for *i = 1 to number-of-plies* and *j = 1 to number-of-bays* to update the orientations and ply-thicknesses of the laminate of each bay. The procedure to generate such a *python-script* is discussed in [5].

3.2. Optimization algorithm

The algorithm starts with a generalized FE model with $[\pm45, (0, 90, \pm45)_4]$ lamination, which is sufficiently strong laminate having positive MOS in all design load cases. The FE model has *J* number of bays (see Fig. 1) and *I* number of variable plies. The initial thickness and orientation details are stored in [TORG] and [AORG] arrays at this stage. The random mutation block of algorithm randomly converts $D_P\%$ thickness values in [TORG] to 0.001 mm by starting with the first bay i.e. *J* = 1. The arrangement is copied to subsequent bays followed by PM as shown by PM block of Fig. 6. The PM program shifts the internal plies towards the external (aerodynamically exposed) ply, whenever the laminate finds a PD during iterative process. The updated lamination is submitted to FE solver by an internal function *SOLVE*. The *SOLVE* function works with orientation and thickness information of lamination to evaluate the fitness function over all the load cases under study. If the obtained solution for the submitted lamination is of better fitness value, then lamination information recorded in [TORG] and [AORG] are updated. The process is repeated *ITP* times. As the solution progresses, fitness function experiences continuous improvement towards a converging solution. The flow diagram shown in Fig. 6 has an internal function *SOLVE*, which submits the arrays [*T*], [*PLYOR*] to

1st Bay	2nd Bay	3rd Bay	4th Bay	5th Bay	6th Bay	7th Bay	8th Bay	9th Bay
0	0	0	0	0	0	0	0	0
90	90	90	90	90	90	90	90	90
+45	+45	+45	+45	+45	+45	+45	+45	+45
-45	-45	-45	-45	-45	-45	-45	-45	-45
0	0	0	0	0	0	0	0	0
90	90	90	90	90	90	90	90	90
+45	+45	+45	+45	+45	+45	+45	+45	+45
-45	-45	-45	-45	-45	-45	-45	-45	-45
0	0	0	0	0	0	0	0	0
90	90	90	90	90	90	90	90	90
+45	+45	+45	+45	+45	+45	+45	+45	+45
-45	-45	-45	-45	-45	-45	-45	-45	-45

ORIGINAL STRING

(a)

1st Bay	2nd Bay	3rd Bay	4th Bay	5th Bay	6th Bay	7th Bay	8th Bay	9th Bay
0	0	0	0	0	0	0	0	0
90	90	90	x	x	x	x	x	x
+45	+45	+45	+45	+45	+45	+45	+45	+45
-45	-45	-45	-45	-45	-45	-45	-45	-45
0	0	0	0	0	0	0	0	0
90	90	90	90	90	90	90	90	90
+45	+45	+45	x	x	x	x	x	x
-45	-45	-45	-45	-45	-45	-45	-45	-45
0	0	0	0	0	0	0	0	0
90	90	90	90	90	90	90	90	90
+45	+45	+45	+45	+45	+45	+45	+45	+45
-45	-45	-45	-45	-45	-45	-45	-45	-45

MUTED STRING

(b)

Fig. 4. Mutation representation (a) Initial laminate (b) Laminate after PD.

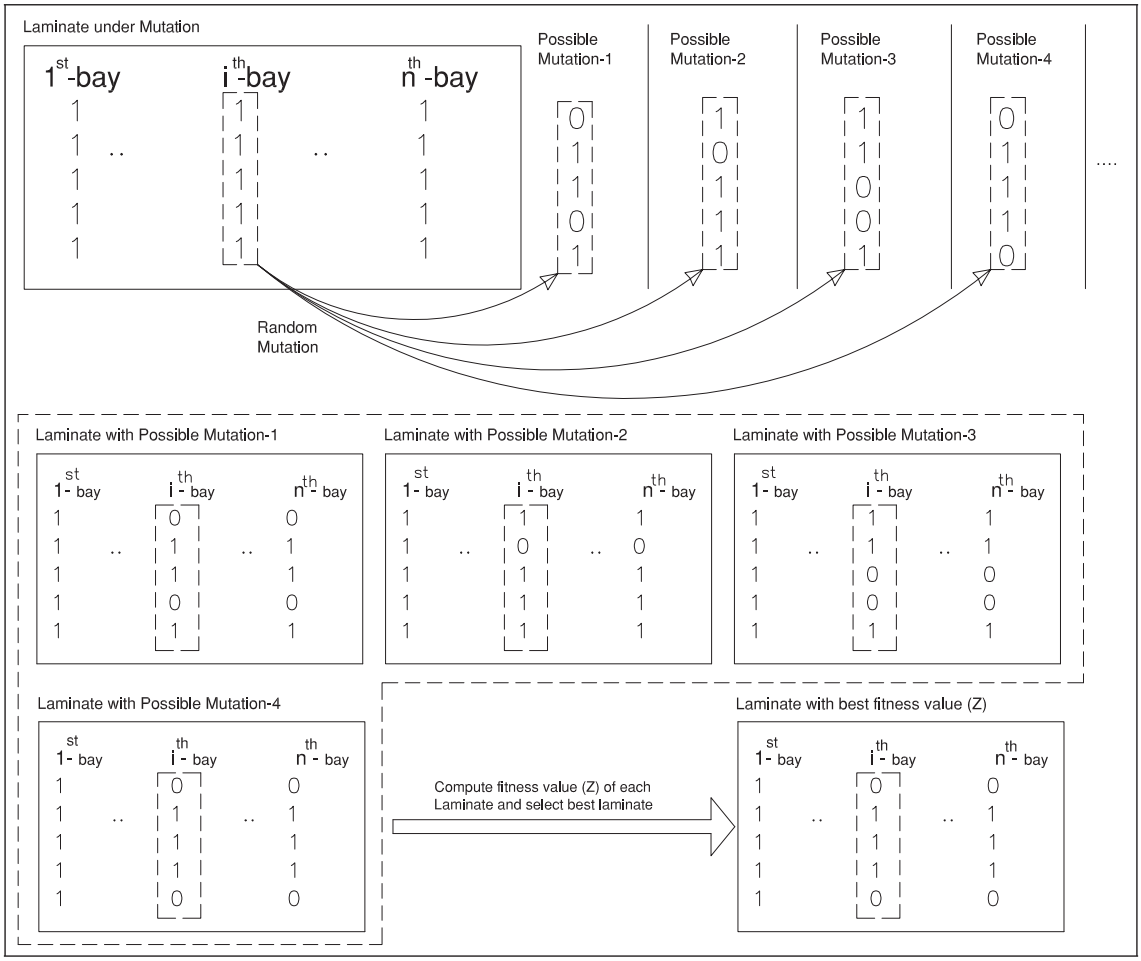

Fig. 5. Formation of chromosomes by random-mutations.

Table 1
Python-script for interface MATLAB with ABAQUS for *k*th LC.

1.	import section	# import ABAQUS environment
2.	execfile('…/inputPD.py')	# import parametric values
3.	openMdb(pathName='…/WING.cae')	# open FE model
4.	p = mdb.models['$wing_k$'].parts['$PART_i$'] region$_i$ = p.sets['P_i']	# read lamination details
	compositeLayup = mdb.models['$wing_k$'].parts['PART-i'].compositeLayups['PANELS$_i$']	for i = 1 to 16 and j = 1 to 15
	compositeLayup.CompositePly(suppressed = False, plyName='Ply-i', region=region$_i$,	
	material='MATERIAL', thicknessType = SPECIFY–THICKNESS, thickness=T_{ij}, …	
	orientationType = SPECIFY–ORIENT, orientation=PLYOR$_{ij}$, axis = AXIS–3, …	
	angle = 0,additionalRotationField='', additionalRotationType = …)	
	ROTATION–ANGLE, numIntPoints = 3	
5.	a = mdb.models['Job-1'].rootAssembly	
6.	mdb.jobs['wingS'].submit(consistencyChecking = OFF)	# submission to solver
7.	mdb.jobs['wingS'].waitForCompletion()	# wait for completion
8.	o3 = session.openOdb('name = …/wingS.odb')	# start result session
9.	odb = session.odbs['…/wingS.odb']	# open result file
11.	session.fieldReportOptions.setValues(printXYData = OFF, printTotal = OFF)	# setting of report format
	session.writeFieldReport(fileName='D:/…/*RESULTS_STATIC*	
	sortItem='Node Label', odb = odb, step = 0, frame = 1, outputPosition = NODAL, …	
	variable=(('U', NODAL, ((INVARIANT, 'Magnitude'),)), ('SDV1', …	
	INTEGRATION–POINT),))	
12.	mdb.jobs['wingB'].submit(consistencyChecking = OFF)	# submission to solver
13.	mdb.jobs['wingB'].waitForCompletion()	# wait for completion
14.	o3 = session.openOdb('name = …/wingB.odb')	# start result session
15.	odb = session.odbs['…/wingB.odb']	# open result file
16.	session.fieldReportOptions.setValues(printXYData = OFF, printTotal = OFF)	# setting of report format
	session.writeFieldReport(fileName='D:/…/*RESULTS_BUCKLING*)	
	sortItem='Node Label', odb = odb, step = 0, frame = 1, outputPosition = NODAL, …	
	variable=(('U', NODAL, ((INVARIANT, 'Magnitude'),))),	
17.	mdb.save(), sys.exit()	# save and exit

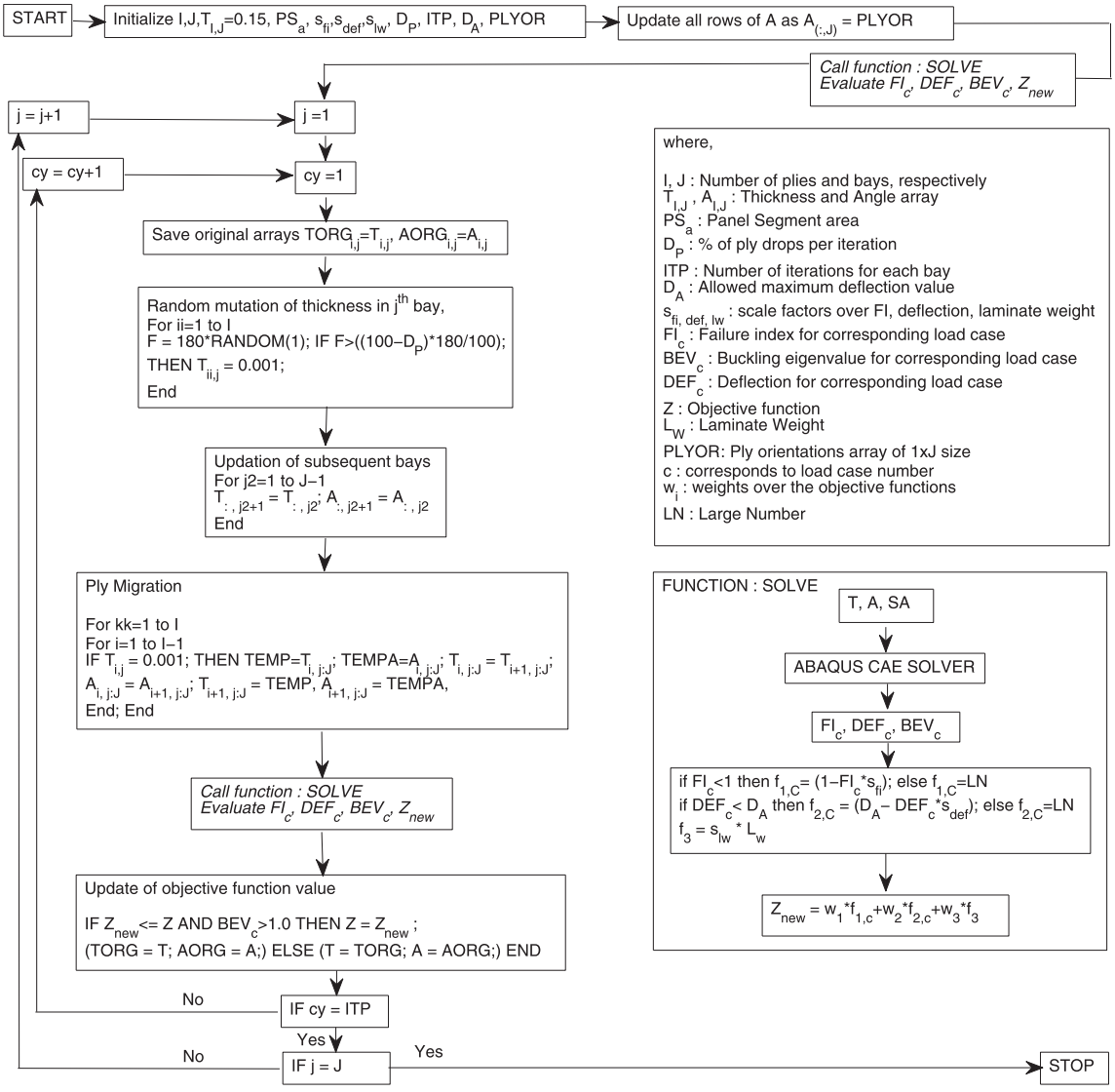

Fig. 6. Flow diagram of optimization process.

ABAQUS/CAE solver using python-script to evaluate FI_c, λ_c and DEF_c for FE model for different load cases.

4. WB optimization

4.1. Construction and loading

The algorithm discussed in Section 3.2 is implemented to optimize WB of a typical fourth generation fighter aircraft [23]. The geometry considered is assumed to have typical three spar construction with basic performance data of the aircraft shown in Table 2. Using this data, basic size of the WB elements have been chalked out by following the procedure given by Howe [24]. The design was based on properties of high strength aluminium alloy with yield strength and elastic modulus of the order of 460 MPa and 69000 MPa, respectively. The basic design was used as an initial design of WB for the demonstration of the procedure. The design was verified using ABAQUS/CAE software to meet deflection, stress and buckling requirements for both LC. Therefore, the initial structure selected was a marginally strong initial candidate with 0.08 and 0.45 MOS in static strength and lateral deflection, respectively.

The two representative aerodynamic load cases for the present study were considered based on high subsonic (M = 0.75) and high supersonic (M = 2.0) chordwise pressure distributions for NACA 6% air-foil [25], which corresponds to forward centre of pressure and rear centre of pressure at 26% and 50%, respectively as shown by Fig. 7. However, the span-wise distribution was a triangular pressure distribution for both the load cases [26]. The C_p distribution over the airfoil was obtained

Table 2
Aircraft basic data [23] and initial size of WB.

Basic aircraft data		Metallic wing box basic size	
Length	21.9 m	Design Load on each Wing	672 kN
Wing Span	4.7 m	Spar Height at Wing Root/Tip	290/100 mm
Height	5.92 m	Spar Web/Flange Thickness	4.5/10 mm
Wing Area	62 m^2	Spar Flange Length	90 mm
Max take-off weight	30,450 kg	Rib Pitch (at root/tip end)	520/260 mm
Engine thrust	122.5 kN	Panel Thickness	3 mm
Max. Speed	2.3 Mach	Number of Ribs	16
Chord length wing root (mm)	3230	Rib Thickness	3 mm
Chord length wing tip (mm)	1290		

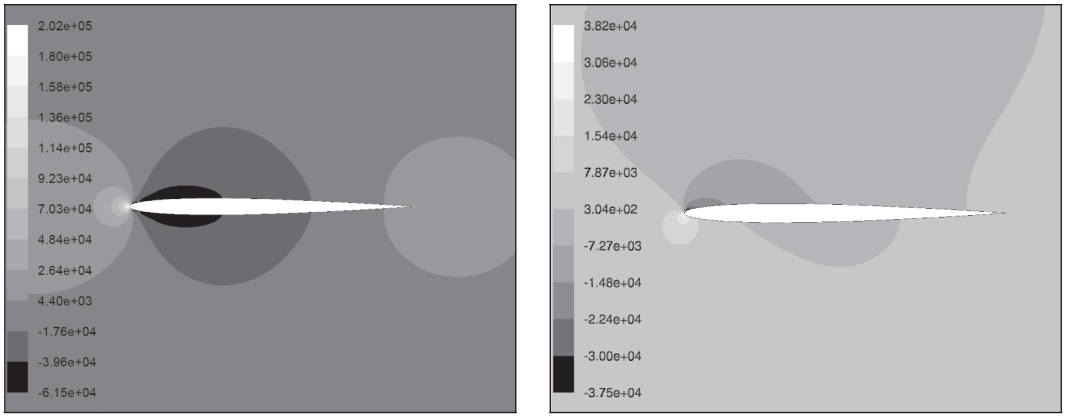

Fig. 7. Airflow over airfoil (a) Subsonic flow $LC{-}1$ (b) Supersonic flow $LC{-}2$.

from *NACA-0006* four digit airfoil. The air flow was studied by 2D CFD analysis using ANSYS software and idealized pressure distribution was followed to apply design load of 672 kN over the WB. The CFD analysis details are not much discussed here as they were beyond the scope of this study.

4.2. Initial FE model

The global FE model of WB for the present study has front, middle and rear spars, ribs, panel-stiffeners and top/bottom panels as major elements. The basic construction and size details of metallic WB are presented in Fig. 8 and Table 2, respectively. The initial design of WB was a high strength aluminium alloy sheet metal construction. The sheet metal elements of WB were then replaced by equivalent quasi-isotropic laminates based on Eqs. (6)–(8) to form initial FE model,

$$[\overline{Q}(\theta)] = [T_1(\theta)]^{-1}[Q][T_2(\theta)] \tag{6}$$

where, $[Q]$ is reduced stiffness matrix, $[T_1(\theta)]$ and $[T_2(\theta)]$ are transformation matrices. In terms of lamina thickness and $[\overline{Q}(\theta)]$, the extensional stiffness matrix $[A]$ for a laminate is given as,

$$\left[A\right] = \frac{1}{h}\sum_{i=1}^{n}\left[\overline{Q}\left(\theta_i\right)\right]\left(t_k - t_{k-1}\right) \tag{7}$$

where, t_k, t_{k-1} are the kth lamina top, bottom co-ordinates from the mid plane, n is the number of layers and h is the total thickness of the laminate (see Herakovich [18]). The compliance matrix is then written as,

$$[S]_{laminate} = [A]^{-1} \tag{8}$$

For a laminate to be a quasi-isotropic, its extensional matrix should have $A_{11} = A_{22}$, $A_{16} = A_{26} = 0$ and $A_{66} = \frac{A_{11} - A_{12}}{2}$. The lamina properties considered for the present analysis are of commerically available prepregs [27], listed in Table 3. The quasi-isotropic laminae in set of 0°, ±45°, 90° were used to replace the sheet metal elements of WB. The thickness and weight details of laminated WB are given in Table 4.

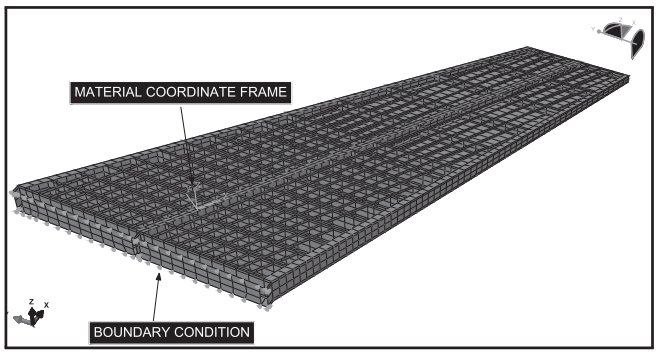

Fig. 8. WB FE Model (panel not shown).

Table 3
Lamina properties [27].

Youngs moduli (E_1, E_2)	164000, 10400 MPa
Poisson's ratio (ν_{12}, ν_{23})	0.24, 0.63
Shear moduli (G_{12})	6354 MPa
Axial tensile/compressive strength (X_t, X_c)	2538, −1483 MPa
Transverse tensile/compressive strength (Y_t, Y_c)	64, −100 MPa
Shear strength in 23, 13 and 12 plane (Q, R, S)	100 MPa

Table 4
Laminate WB element details.

Element	Uniform Thickness (mm)	Weight (kg)	Plies
Top Panel	5.4	94.6	36
Bottom Panel	5.4	94.6	36
Front Spar	5.4	17.1	36
Middle Spar	5.4	17.7	36
Rear Spar	5.4	15.2	36
Ribs	3.6	46.1	24
Panel Stiffeners	3.6	21.3	24

4.3. WB FE model

The FE model of WB along with material coordinate system for panel laminates is shown in Fig. 8. It has 6253 S4 4-noded and 24 S3 3-noded general purpose shell elements. The element used has 6 DOF and works with reduced stiffness matrix with finite strain. The shell elements of ABAQUS are well suited for 3D FE modeling of planar sections. A complete generalized material model along with freedom to change material orientations is supported in the FE model.

The computation of stresses, deflection, buckling eigenvalue λ for the FE model is possible in CAE software like ABAQUS. The formulation involved are discussed in Section 4.5 and 4.6. The laminates of the WB were defined in ALM. The number of layers for the initial FE model considered for the WB members were in accordance with Table 4. The panel laminate for this problem was discretized in 15 piece-wise laminates, with each set of laminate extending between adjacent ribs to form bays. The set of laminates behaves as a single laminate during analysis by virtue of continuity of plies in SS in adjacent bays. The ply-orientation and thickness parameters of each bay lamination were externally controllable by algorithm using *python-scripting*. During optimization, the algorithm alters the thickness and orientation variables of

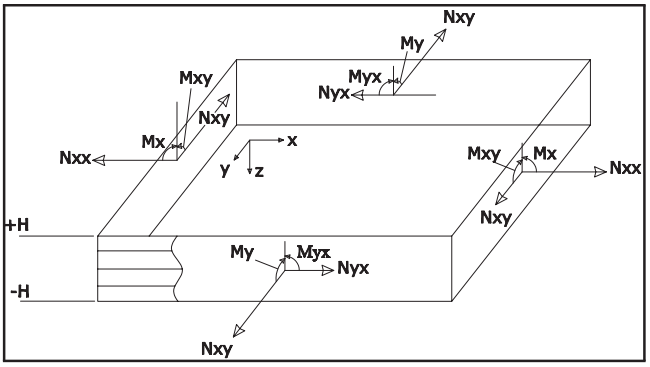

Fig. 9. Laminate showing stress resultants.

lamination. The FE model with altered variables is then solved for different load cases for evaluation of deflection, buckling and strength.

Since, the wing is an aerodynamic surface, the PD on air exposed surface has to be avoided and plies are dropped internally [12]. To achieve this, top/bottom layers with $[\pm 45]_s$ known as cover plies [7], are maintained over the laminates. The requirement of maintaining smooth surface on air-exposed side along with symmetry of laminates is maintained by migrating the plies towards external face and symmetrically dropping the plies internally during optimization.

4.4. Boundary condition

The boundary condition to this FE model is assigned as in-plane translation constraint to panel laminates and spar webs at the wing-root as shown in Fig. 8.

4.5. Laminate stress analysis

Stresses and displacements in each layer of the laminate are calculated by classical laminate theory (CLT) [18]. In CLT, each lamina is in planar state of stress and shear strains γ_{zx} and γ_{zy} are identically zero. Therefore, the z displacement is a function of x and y coordinates only. The in-plane strain at any z location is given as

$$\begin{Bmatrix} \varepsilon_x \\ \varepsilon_y \\ \gamma_{xy} \end{Bmatrix} = \begin{Bmatrix} \varepsilon_x^0 \\ \varepsilon_y^0 \\ \gamma_{xy}^0 \end{Bmatrix} + z \begin{Bmatrix} \kappa_x \\ \kappa_y \\ \kappa_{xy} \end{Bmatrix} \tag{9}$$

where, $\{\varepsilon^0\}$ are mid-plain strains and $\{\kappa\}$ are mid-plane curvatures. The in-plane forces per unit length $\{N\}$ in the laminate thickness are defined by the integral of planar stresses as (see Fig. 9).

$$\{N\} = \int_H^{-H} \{\sigma\} dz \tag{10}$$

In terms of transformed reduced stiffness matrix, the Eq. (10) for the k_{th} layer will be

$$\{N\} = \int_H^{-H} [\overline{Q}]^k \{\varepsilon^0\} dz + \int_H^{-H} [\overline{Q}]^k \{\kappa\} z\, dz \tag{11}$$

Similarly, for out-of-plane moments per unit length, $\{M\}$ is written as,

$$[M] = \int_H^{-H} [\overline{Q}]^k \{\varepsilon^0\} z\, dz + \int_H^{-H} [\overline{Q}]^k \{\kappa\} z^2\, dz \tag{12}$$

Combining Eq. (11) and Eq. (12),

$$\begin{Bmatrix} N \\ M \end{Bmatrix} = \begin{bmatrix} A & B \\ B & D \end{bmatrix} \begin{Bmatrix} \varepsilon^0 \\ \kappa \end{Bmatrix} \tag{13}$$

where, $[A] = \sum_{k=1}^{N} (Z_k - Z_{k-1})$, $\left[B\right] = \frac{1}{2} \sum_{k=1}^{N} [\overline{Q}]^k \left(Z_k^2 - Z_{k-1}^2\right)$, $\left[D\right] = \frac{1}{3} \sum_{k=1}^{N} [\overline{Q}]^k \left(Z_k^3 - Z_{k-1}^3\right)$. Further, the Eq. (13) can be rearranged as,

$$\begin{Bmatrix} \varepsilon^0 \\ \kappa \end{Bmatrix} = \begin{bmatrix} A' & B' \\ B'^T & D' \end{bmatrix} \begin{Bmatrix} N \\ M \end{Bmatrix} \tag{14}$$

where, $[A'] = [A]^{-1} + [A]^{-1}[B][D^*]^{-1}[B][A]^{-1}$, $[B'] = -[A]^{-1}[B][D^*]^{-1}$, $[D'] = ([D] - [B][A]^{-1}[B])^{-1}$ and $[D^*] = [D] - [B][A]^{-1}[B]$. Now, with known values of in plane strains and curvatures the stress state can be derived as,

$$\{\sigma\}^k = [\overline{Q}]^k \{\varepsilon^0\} + [\overline{Q}]^k z \{\kappa\} \tag{15}$$

The Eq. (15) is computed in ABAQUS/CAE to evaluate laminate stress distribution.

4.6. Buckling analysis

The buckling predictions for present optimization has been carried out using ABAQUS CAE. The ABAQUS uses Lancoz linear eigensolver to obtain critical buckling mode. In an eigenvalue analysis, nominal load is applied to the linear perturbation procedure. The analysis step involving linear perturbation evaluates the eigenvalues and multiply it with applied loading to predict buckling loads. The analysis step also determines the eigenvectors for the subject problem, in which the applicable loads can be concentrated forces, pressures, prescribed displacements, thermal loading. The eigenvalue (λ) obtained in buckling analysis gives the reserve factor in buckling for the applied loads on structure. In present study, the analysis has been carried out on FE model having S4 4-noded and S3 3-noded general purpose shell elements [28,7,13].

5. Results and discussions

This section deals with results of the application of PD algorithm to a WB design. Out of the seven important structural members (see Table 4), panel optimization has been selected in present study as it has maximum contribution towards assembly weight. However, it is possible to apply the study for optimization of WB spars also. The FE model with panel laminate having 16 symmetric variable plies along with 2 top and 2 bottom fixed layers (cover plies) was submitted by MATLAB, based on flow diagram of Fig. 6 to ABAQUS FE solver. The section also discusses about selection of weight vector w_i of fitness function discussed in Section 2.4, which plays an important role in deciding design objective to be optimized.

5.1. Selection of weight vector

The w_i selection for obtaining optimal results has been made based on *a posteriori* articulation [22,29]. As an *a posteriori* articulation, the optimization problem was solved with different choices of w_i as given in Table 5. The w_1 choices considered in Table 5 were in increments of 0.1, however w_2 and w_3 were output of a random number generator such that $\sum_{i=1}^{3} w_i = 1$. The scaling factors s_{fi}, s_{def} and s_{tw} were estimated using Eq. (5) as 189.2, 0.63 and 1.0, respectively on the basis of s_{tw}. The initial FE model submitted for optimization had uniform panel thickness (5.4 mm). The panel laminate had symmetric SS of 16 variable plies and 2 fixed plies for the 15 bays. Therefore, the entire laminate is considered as a set of 15 piecewise laminates in the FE model. For the present study, iterations per bay (*ITP*) is considered as 16, therefore, optimizer will perform 16 iterations for optimization of each bay, in which random mutation operator will randomly select plies of quasi-isotropic laminate to form new chromosomes. The problem was submitted to solver for different cases of w_i with $\delta_a = 300$ mm, $FI \leq 1.0$ and $\lambda \geqslant 1$. The resulting values of FI, δ, λ and L_w for the all (two) LCs are tabulated in Table 5.

The results obtained show that, the solutions are bounded, i.e. the values FI, δ and λ for all the load-cases are within the constraints as expected with Eq. (4). The results obtained after solutions of cases mentioned in Table 5 are shown on scatter plots of Fig. 10. The scatter

Table 5
Results with w_i choices for two load cases.

					Load case-1			Load case-2		
Case	w_1	w_2	w_3	L_w(kg)	*FI*	δ(mm)	λ	*FI*	δ(mm)	λ
1	0.900	0.066	0.035	111.800	0.946	233.730	1.225	1.000	233.494	1.340
2	0.900	0.094	0.006	117.825	0.934	253.030	1.130	1.000	249.900	1.245
3	0.900	0.092	0.008	111.772	0.943	240.279	1.086	0.999	240.279	1.186
4	0.900	0.094	0.007	113.802	0.948	239.543	1.154	1.000	240.073	1.325
5	0.900	0.088	0.012	121.502	0.957	235.265	1.132	1.000	232.910	1.240
6	0.800	0.120	0.080	91.080	0.918	262.763	1.001	0.999	263.380	1.081
7	0.800	0.165	0.035	87.590	0.886	299.071	1.005	0.986	296.236	1.082
8	0.800	0.096	0.104	93.605	0.929	248.654	1.019	1.000	248.194	1.244
9	0.800	0.057	0.143	90.578	0.926	258.076	1.067	1.000	259.519	1.282
10	0.800	0.084	0.116	98.365	0.939	252.477	1.017	1.000	252.594	1.256
11	0.700	0.048	0.252	115.600	0.922	236.056	1.006	1.000	230.616	1.217
12	0.700	0.030	0.270	114.880	0.940	233.034	1.004	1.000	231.590	1.226
13	0.700	0.244	0.056	87.222	0.923	278.844	1.016	1.000	279.016	1.259
14	0.700	0.293	0.007	93.046	0.918	274.557	1.028	1.000	273.892	1.179
15	0.700	0.048	0.252	104.508	0.938	238.085	1.001	1.000	237.945	1.224
16	0.600	0.252	0.148	89.612	0.931	266.208	1.000	0.989	267.200	1.086
17	0.600	0.283	0.117	90.407	0.931	256.740	1.014	1.000	257.382	1.262
18	0.600	0.326	0.074	87.222	0.923	278.844	1.016	1.000	279.016	1.259
19	0.600	0.390	0.010	86.930	0.913	282.200	1.014	0.999	281.731	1.180
20	0.600	0.340	0.060	84.610	0.916	298.923	1.005	0.999	299.110	1.113
21	0.500	0.407	0.093	87.222	0.923	278.844	1.016	1.000	279.016	1.259
22	0.500	0.485	0.015	87.385	0.917	283.012	1.001	0.991	278.786	1.265
23	0.500	0.080	0.420	104.508	0.938	238.085	1.001	1.000	237.945	1.224
24	0.500	0.012	0.488	95.843	0.935	241.848	1.003	1.000	242.813	1.213
25	0.500	0.488	0.012	86.381	0.916	281.095	1.016	1.000	279.776	1.179
26	0.400	0.489	0.111	87.222	0.923	278.844	1.016	1.000	279.016	1.250
27	0.400	0.586	0.015	86.380	0.916	281.095	1.016	1.000	279.776	1.179
28	0.400	0.096	0.504	104.508	0.938	238.085	1.001	1.000	237.945	1.224
29	0.400	0.551	0.049	89.686	0.929	257.380	1.039	0.999	256.450	1.273
30	0.400	0.348	0.253	94.689	0.943	256.309	1.002	1.000	254.310	1.223
31	0.300	0.112	0.588	104.508	0.938	238.085	1.001	1.000	237.945	1.224
32	0.300	0.017	0.683	95.843	0.935	241.840	1.003	1.000	242.813	1.213
33	0.300	0.405	0.295	107.801	0.943	256.309	1.018	1.000	254.310	1.223
34	0.300	0.519	0.182	86.340	0.928	299.772	1.002	0.994	299.429	1.155
35	0.300	0.175	0.525	91.600	0.928	256.181	1.029	1.000	256.185	1.277
36	0.200	0.593	0.207	93.479	0.928	299.772	1.002	0.994	299.429	1.155
37	0.200	0.200	0.600	91.605	0.928	256.181	1.029	1.000	256.185	1.277
38	0.200	0.198	0.602	94.758	0.945	250.096	1.032	1.000	249.539	1.223
39	0.200	0.702	0.098	100.728	0.938	246.179	1.001	1.000	247.246	1.223
40	0.200	0.474	0.326	97.708	0.929	265.223	1.000	0.982	265.320	1.090

plots are for critical values of the two load cases between *FI*, δ vs L_w. The dotted line in the Fig. 10 shows front formed by non-dominated solutions. Since, the problem is focussed towards the laminate weight optimization, the Cases 7, 13, 18–22, 25–27 and 34 are of interest, in which the results are near global optimal, i.e. laminate weight L_w is less than 88.0 kg. The points correspond to bottom-most points on the scatter plot as shown by the dotted circle in Fig. 10. In these solutions, the laminate weight is minimum along with minimum positive MOS in design criteria. Out of these cases, the minimum weight is obtained for Case 20, in which the MOS for FI and lateral deflection is 0.001 and 0.003, respectively, which indicates that the results are near to global optima. Taking guideline from the weight vectors w_i of Cases 7, 13, 18–22, 25–27 and 34, the selection of w_i is made as $(0.45,\ 0.45,\ 0.1)^T$. The selected w_i has w_1 and w_2 with equal values and it is higher than the value of w_3. This enforces the algorithm to optimize the design criteria at higher priority. Since, the present algorithm includes selection of random plies while optimization, the problem was submitted to optimizer for multiple times with selected value of w_i. The results obtained demonstrate the consistency of optimizer and achievement of a better result in the search process. The results obtained are discussed in next section.

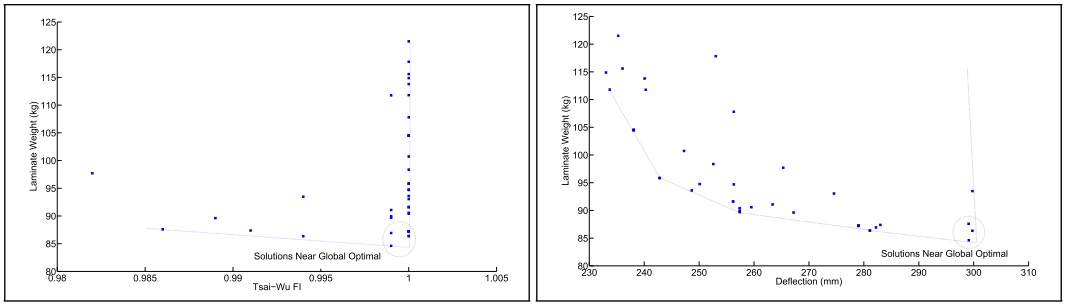

(a) (b)

Fig. 10. Scatter plot (a) Laminate weight vs Tsai Wu FI (b) Laminate weight vs deflection.

Table 6
Repeatability test results

		LC-1			LC-2		
Submission No.	Laminate Weight (kg)	FI	δ	λ	FI	δ	λ
1	81.4783	0.9523	293.3550	1.0104	0.9983	294.9930	1.0959
2	86.7725	0.9321	282.8520	1.0010	0.9952	284.1070	1.0853
3	83.1477	0.9337	280.6930	1.0132	0.9979	283.0400	1.0968
4	91.9653	0.9293	265.5723	1.0062	0.9999	267.1216	1.1301
5	81.4783	0.9523	293.3550	1.0104	0.9983	294.9930	1.0959
6	86.7725	0.9321	282.8520	1.0010	0.9952	284.1070	1.0853
7	83.1477	0.9332	2806930	1.0132	0.9979	283.0400	1.0968
8	86.7725	0.9321	282.8520	1.0010	0.9952	284.1070	1.0853

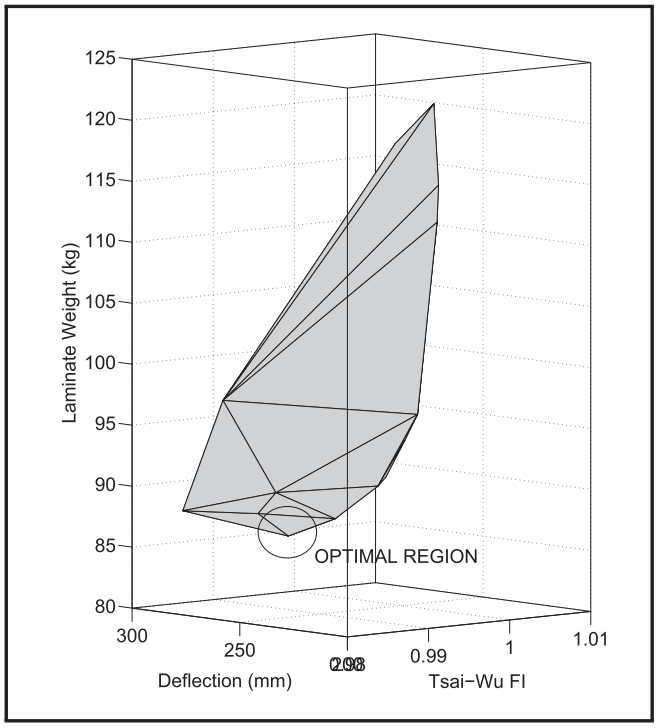

Fig. 11. Results 3D-hull plot.

5.2. Optimization results

Since the algorithm involves random selection of plies, the check for the consistency of results with selected w_i has been carried out. Therefore, the problem was submitted to optimizer for 8 times with w_i as $(0.45, 0.45, 0.1)^T$ and rest of the parameters as discussed in Section 5.2. The results obtained from multiple submission are placed at Table 6. The results show that seven out of eight times the optimizer reached close to global optimal value, whereas only for one submission optimizer got stuck at some local optima.

The solutions obtained in Table 5 have been used as data set to develop a n-dimensional convex hull plot with critical values of FI, L_w and δ out of the two load cases. The bottom most points of plot correspond to region of optimal solutions where one can see laminate weight is minimum while design criteria are in acceptable limits. The outer envelop of Fig. 11 has a convex appearance, which shows that the problem is suitable for *a posteriori* articulation. The plots shown in Fig. 12 gives an insight to optimization process. The points obtained between MOS of design criteria vs laminate weight during optimization process show that the solutions have positive MOS in the entire optimization process. The Fig. 12 also shows weight minimization at the cost of reduction in MOS, i.e. initially laminate weight, which was close to 189 kg, got reduced by 110 kg with utilization of excess MOS.

After optimization, from Table 7 it can be seen that ply 4, 8 and 17 are completely dropped out from the laminate in the iteration of first bay itself. The PD in the first bay is accompanied by removal of plies from subsequent bays also. The iterations for the second bay brought out drop of 6th ply. Similarly, iteration for the tenth bay brought out drop of 5th ply. The stepwise dropping of plies at the end of iterations resulted in the formation of (see Table 7) an upper-triangular shape, which is equivalent to a tapered laminate, tapering from root to tip. The Table 7, also shows pileup of laminae towards the external aerodynamic surface during optimization, which was a design feature of the algorithm.

As the solution progresses, penalties for the deviations from the design values can be monitored as spikes in Fig. 13. The *FI* spikes can be seen in the initial generations of Fig. 13 and corresponding exceedance of *FI* allowable in Fig. 14. Similarly, one can see lateral deflection penalties in Fig. 13 and corresponding exceedance in δ in Fig. 14. The penalty plots (Fig. 13) show zero value when the design criteria are within the acceptable limits. In case of multi-load case analysis, where hundreds of design load cases are involved, the monitoring of plots in Fig. 13 shows the critical design parameter in each generation.

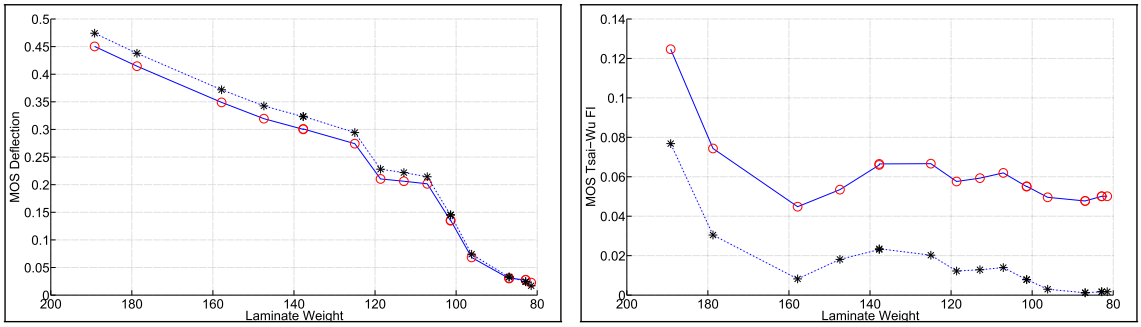

(a) (b)

Fig. 12. Case-1,5 MOS plots for LC-1 (∘) and LC-2 (∗) (a) MOS Deflection vs Panel Weight (b) MOS Tsai-Wu FI vs Panel Weight.

Table 7
Laminate variables after nth-bay optimization.

Ply/Bay	1	2	3	4	5	6	7	8	9	10	11	12	13	14	15
Initial Laminate															
3	0	0	0	0	0	0	0	0	0	0	0	0	0	0	0
4	90	90	90	90	90	90	90	90	90	90	90	90	90	90	90
5	45	45	45	45	45	45	45	45	45	45	45	45	45	45	45
6	−45	−45	−45	−45	−45	−45	−45	−45	−45	−45	−45	−45	−45	−45	−45
7	0	0	0	0	0	0	0	0	0	0	0	0	0	0	0
8	90	90	90	90	90	90	90	90	90	90	90	90	90	90	90
9	45	45	45	45	45	45	45	45	45	45	45	45	45	45	45
10	−45	−45	−45	−45	−45	−45	−45	−45	−45	−45	−45	−45	−45	−45	−45
11	0	0	0	0	0	0	0	0	0	0	0	0	0	0	0
12	90	90	90	90	90	90	90	90	90	90	90	90	90	90	90
13	45	45	45	45	45	45	45	45	45	45	45	45	45	45	45
14	−45	−45	−45	−45	−45	−45	−45	−45	−45	−45	−45	−45	−45	−45	−45
15	0	0	0	0	0	0	0	0	0	0	0	0	0	0	0
16	90	90	90	90	90	90	90	90	90	90	90	90	90	90	90
17	45	45	45	45	45	45	45	45	45	45	45	45	45	45	45
18	−45	−45	−45	−45	−45	−45	−45	−45	−45	−45	−45	−45	−45	−45	−45
1st-Bay Optimization															
3	0	0	0	0	0	0	0	0	0	0	0	0	0	0	0
4	45	45	45	45	45	45	45	45	45	45	45	45	45	45	45
5	0	0	0	0	0	0	0	0	0	0	0	0	0	0	0
6	90	90	90	90	90	90	90	90	90	90	90	90	90	90	90
7	45	45	45	45	45	45	45	45	45	45	45	45	45	45	45
8	0	0	0	0	0	0	0	0	0	0	0	0	0	0	0
9	90	90	90	90	90	90	90	90	90	90	90	90	90	90	90
10	−45	−45	−45	−45	−45	−45	−45	−45	−45	−45	−45	−45	−45	−45	−45
11	0	0	0	0	0	0	0	0	0	0	0	0	0	0	0
12	90	90	90	90	90	90	90	90	90	90	90	90	90	90	90
13	45	45	45	45	45	45	45	45	45	45	45	45	45	45	45
14	−45	−45	−45	−45	−45	−45	−45	−45	−45	−45	−45	−45	−45	−45	−45
15	×	×	×	×	×	×	×	×	×	×	×	×	×	×	×
16	×	×	×	×	×	×	×	×	×	×	×	×	×	×	×
17	×	×	×	×	×	×	×	×	×	×	×	×	×	×	×
18	×	×	×	×	×	×	×	×	×	×	×	×	×	×	×
2nd-Bay Optimization															
3	0	0	0	0	0	0	0	0	0	0	0	0	0	0	0
4	45	45	45	45	45	45	45	45	45	45	45	45	45	45	45
5	0	0	0	0	0	0	0	0	0	0	0	0	0	0	0
6	90	45	45	45	45	45	45	45	45	45	45	45	45	45	45
7	45	0	0	0	0	0	0	0	0	0	0	0	0	0	0
8	0	90	90	90	90	90	90	90	90	90	90	90	90	90	90
9	90	−45	−45	−45	−45	−45	−45	−45	−45	−45	−45	−45	−45	−45	−45
10	−45	0	0	0	0	0	0	0	0	0	0	0	0	0	0
11	0	90	90	90	90	90	90	90	90	90	90	90	90	90	90
12	90	45	45	45	45	45	45	45	45	45	45	45	45	45	45
13	45	−45	−45	−45	−45	−45	−45	−45	−45	−45	−45	−45	−45	−45	−45
14	−45	×	×	×	×	×	×	×	×	×	×	×	×	×	×
15	×	×	×	×	×	×	×	×	×	×	×	×	×	×	×
16	×	×	×	×	×	×	×	×	×	×	×	×	×	×	×
17	×	×	×	×	×	×	×	×	×	×	×	×	×	×	×
18	×	×	×	×	×	×	×	×	×	×	×	×	×	×	×
10th-Bay Optimization															
3	0	0	0	0	0	0	45	45	45	45	45	45	45	45	45
4	45	45	45	45	45	45	0	0	−45	0	0	0	0	0	0
5	−45	0	0	0	0	0	−45	−45	90	×	×	×	×	×	×
6	0	45	45	45	45	45	0	90	0	×	×	×	×	×	×
7	45	−45	−45	−45	−45	−45	90	0	×	×	×	×	×	×	×
8	−45	0	0	0	0	0	−45	×	×	×	×	×	×	×	×
9	0	90	90	90	90	90	0	×	×	×	×	×	×	×	×
10	90	−45	−45	−45	−45	−45	−45	×	×	×	×	×	×	×	×
11	−45	0	0	0	0	0	×	×	×	×	×	×	×	×	×
12	0	90	90	90	90	90	×	×	×	×	×	×	×	×	×
13	90	−45	−45	−45	−45	−45	×	×	×	×	×	×	×	×	×
14	−45	×	×	×	×	×	×	×	×	×	×	×	×	×	×
15	×	×	×	×	×	×	×	×	×	×	×	×	×	×	×
16	×	×	×	×	×	×	×	×	×	×	×	×	×	×	×
17	×	×	×	×	×	×	×	×	×	×	×	×	×	×	×
18	×	×	×	×	×	×	×	×	×	×	×	×	×	×	×
11th-Bay Optimization															
3	0	0	0	0	0	0	45	45	45	45	0	0	0	0	0
4	45	45	45	45	45	45	0	0	−45	0	×	×	×	×	×
5	−45	0	0	0	0	0	−45	−45	90	×	×	×	×	×	×

(*continued on next page*)

Table 7 (*continued*)

Ply/Bay	1	2	3	4	5	6	7	8	9	10	11	12	13	14	15
6	0	45	45	45	45	45	0	90	0	×	×	×	×	×	×
7	45	−45	−45	−45	−45	−45	90	0	×	×	×	×	×	×	×
8	−45	0	0	0	0	0	−45	×	×	×	×	×	×	×	×
9	0	90	90	90	90	90	0	×	×	×	×	×	×	×	×
10	90	−45	−45	−45	−45	−45	−45	×	×	×	×	×	×	×	×
11	−45	0	0	0	0	0	×	×	×	×	×	×	×	×	×
12	0	90	90	90	90	90	×	×	×	×	×	×	×	×	×
13	90	−45	−45	−45	−45	−45	×	×	×	×	×	×	×	×	×
14	−45	×	×	×	×	×	×	×	×	×	×	×	×	×	×
15	×	×	×	×	×	×	×	×	×	×	×	×	×	×	×
16	×	×	×	×	×	×	×	×	×	×	×	×	×	×	×
17	×	×	×	×	×	×	×	×	×	×	×	×	×	×	×
18	×	×	×	×	×	×	×	×	×	×	×	×	×	×	×
15th-Bay Optimization															
3	0	0	0	0	0	0	45	45	45	45	0	0	0	×	×
4	45	45	45	45	45	45	0	0	−45	0	×	×	×	×	×
5	−45	0	0	0	0	0	−45	−45	90	×	×	×	×	×	×
6	0	45	45	45	45	45	0	90	0	×	×	×	×	×	×
7	45	−45	−45	−45	−45	−45	90	0	×	×	×	×	×	×	×
8	−45	0	0	0	0	0	−45	×	×	×	×	×	×	×	×
9	0	90	90	90	90	90	0	×	×	×	×	×	×	×	×
10	90	−45	−45	−45	−45	−45	−45	×	×	×	×	×	×	×	×
11	−45	0	0	0	0	0	×	×	×	×	×	×	×	×	×
12	0	90	90	90	90	90	×	×	×	×	×	×	×	×	×
13	90	−45	−45	−45	−45	−45	×	×	×	×	×	×	×	×	×
14	−45	×	×	×	×	×	×	×	×	×	×	×	×	×	×
15	×	×	×	×	×	×	×	×	×	×	×	×	×	×	×
16	×	×	×	×	×	×	×	×	×	×	×	×	×	×	×
17	×	×	×	×	×	×	×	×	×	×	×	×	×	×	×
18	×	×	×	×	×	×	×	×	×	×	×	×	×	×	×

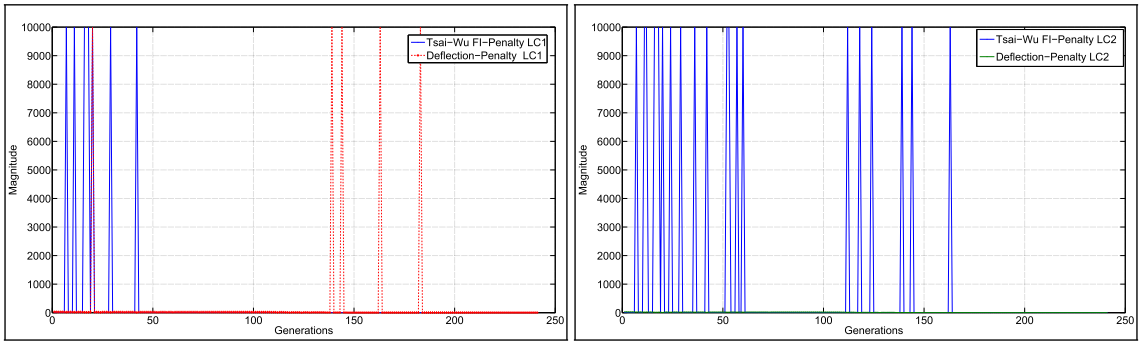

(a) (b)

Fig. 13. Monitoring of penalties for Case-5 (a) LC-1 (b) LC-2.

Therefore, these plots address the design parameter and load case responsible for non-convergence of solution.

The algorithm for present problem is designed in such a way that the deviation of any of the design criteria generate penalty, which prevents the solution to be accepted in the next generation. In this process, if a solution is better, then only it is accepted in the iterative process and its fitness value becomes benchmark for the entry of next solution. The next solution that appears in the iterative process will be

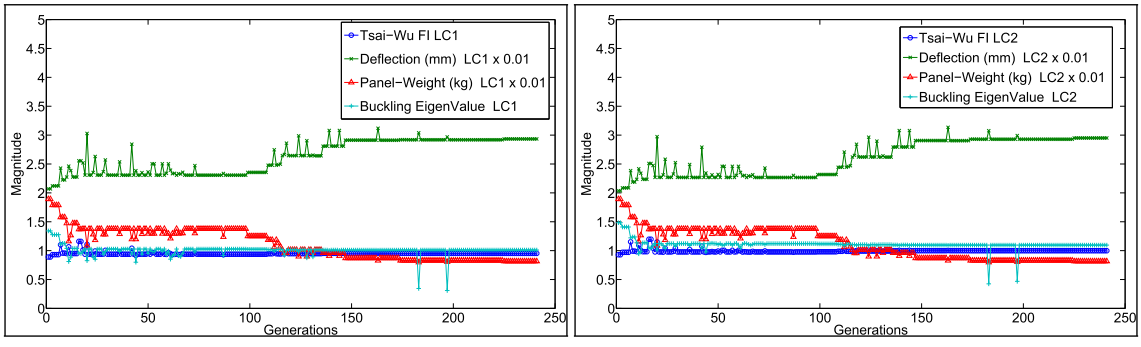

(a) LC-1 (b) LC-2

Fig. 14. Monitoring of solution convergence for Case-5 (a) LC-1 (b) LC-2.

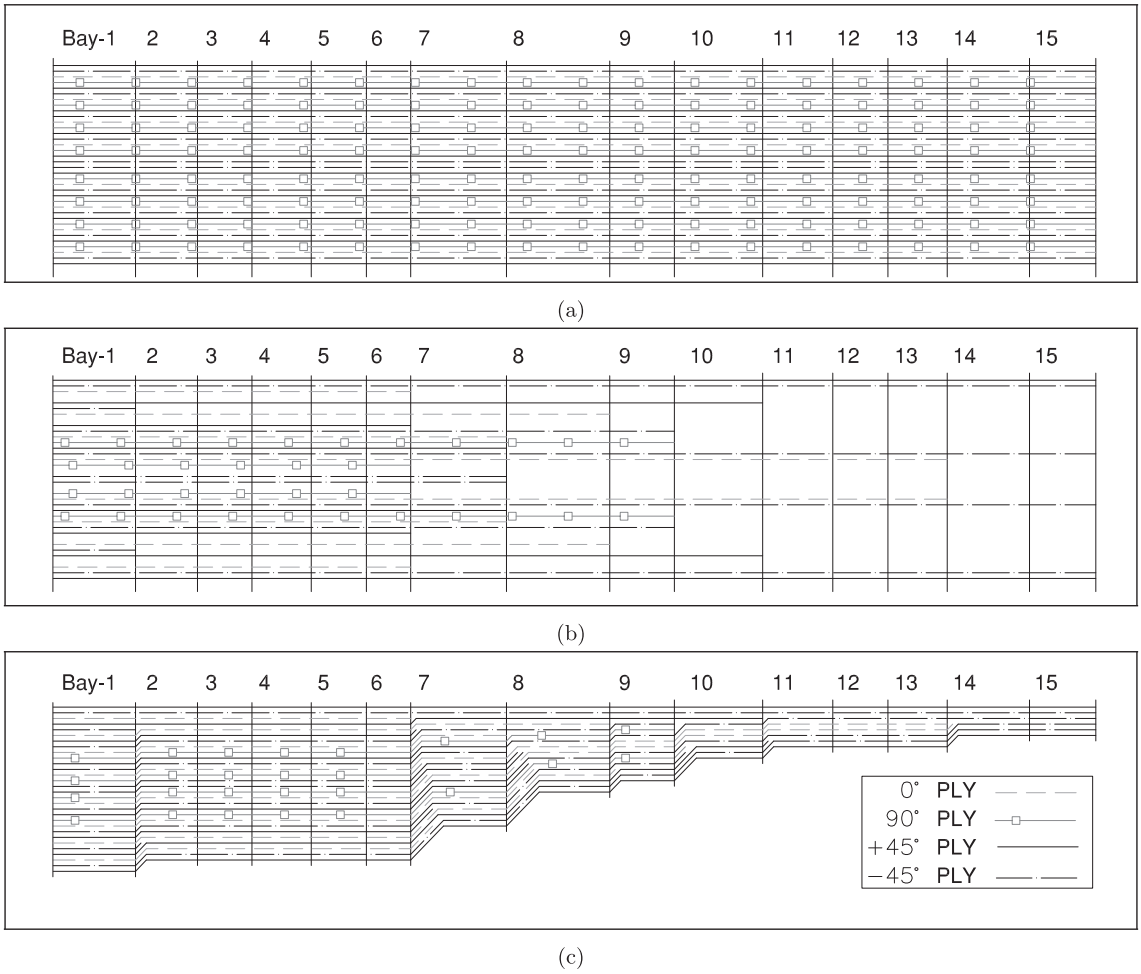

Fig. 15. Top panel laminate (a) Initial laminate (b) Laminate by virtue of PD (c) Laminate after PD and PM.

accepted only if the value of fitness function is better than the previous one. The Fig. 14 shows monitoring of design parameters along with the laminate (panel) weight (top and bottom). The laminate weight was 189 kg at the start of solution, which slowly reduces as the solution progresses. At the end of optimization the weight of panel was 81.4 kg, which is 57% less than the initial weight. During optimization, MOS in *FI* and δ was initially 0.08 and 0.45, respectively, which was utilized towards the weight optimization. The respective MOS safety values after optimization were 0.001 and 0.003, which show MOO in the present problem. Sometimes, less MOS can be mislead as a weak structure, however, it is not the case and it has to be considered that excess MOS doesn't add value to the design. Moreover, if the designer wishes to have more MOS, then the design allowable (target value) can be altered in the present optimizer. Therefore, the beauty of the present optimizer lies in achieving the target value for the design criteria and thereby leaving the minimum MOS.

5.3. Independent solution of FE optimal model

The FE analysis has been carried out for the optimal SS without dummy plies in ABAQUS/CAE and the solution was verified for different load cases and design criteria. The results obtained by the independent FE model solution and those obtained by the algorithm based solution were in close match. The close match indicates that introduction of dummy plies (0.001 mm thickness) within laminate has no adverse affect over the FE model and results are bounded with and without dummy plies [5].

5.4. Lamination

The laminate of top-panel has 4 fixed and 32 variable plies before optimization as shown in Fig. 15a. The variable plies of laminate are formed by 4 sets of quasi-isotropic laminae. As the solution proceeds, plies from quasi-isotropic sets are dropped. The dropped out plies at the end of optimization are shown in Fig. 15b. During solution, ply drop is always associated with the shift (migration) of a ply towards the outer layer. Therefore, laminate formed after PD and PM is shown in Fig. 15c. The laminate obtained after optimization is an acceptable arrangement for manufacturing. During manufacturing, plies which are terminating near the rib axes are dropped down in drop-offset distance. The typical maximum value of drop-offset distance involved in the PD is of the order of 0.5 mm per ply, i.e., 0.2% of rib to rib distance in the present case. Therefore, there will be a smooth blending of dropped plies. The PD is followed by the formation of a small resin-pocket, which is typical in laminate design. The laminate suggested after optimization is a piecewise symmetric laminate in all the bays. However, there is a continuity of plies with neighbouring laminate, which gives continuity to laminate along with full blending. Moreover, the laminate obtained after optimization is piecewise symmetric with smooth external aerodynamic surface.

6. Conclusions

In this study an attempt has been made to design tapered laminates for wing panels of a fighter aircraft by ply-drop. The algorithm developed caters to get optimal ply-drop as well as ply-migration to achieve

blended laminates. The study has been implemented for optimization of a representative typical 3 spar fourth generation fighter aircraft wing geometry. The following are the key conclusions drawn from the study.

(a)The penalty approach followed in the present study imposes double-sided penalty on the fitness function whenever there is a deviation from design criteria. Therefore, the double sided penalty enforces optimizer to attain targeted design values at every generation.
(b)The penalty approach along with suitable weight factors successfully guided fitness-function to select new chromosomes in iterative process. The penalty plots developed were found useful in the identification of load case and design criterion which were responsible for non-convergence in multi-load case design environment.
(c)The study on selection of weight vector w_i over the fitness function showed that priority of w_i should be higher for design criterion than laminate weight so that the optimizer performs weight optimization only when design requirements are fulfilled.
(d)The quasi-isotropic laminate choice as an initial laminate along with the random selection of plies minimized complexities of handling full-fledged GA during optimization.
(e)The optimizer successfully rearranged ply-angles so as to follow the ply-drops within the set of laminates along with backward continuity.
(f)The optimizer performed 23% full length ply-drops and 43% partial length ply-drops, which indicate high effectiveness of the optimization algorithm. After optimization the weight of the panel was reduced to 81.4 kg, which was initially 189 kg.
(g)The algorithm developed brings out optimal ply-termination as well as flow path of plies with minimum positive MOS for all the design load cases under study. After ply-drop, laminates obtained for the panel are piecewise symmetric. Therefore, there will be no inherent bending of laminate.
(h)The optimizer successfully maintained positive MOS for all the load cases and brought out significant amount of weight reduction by the utilization of MOS. The MOS after optimization is in the range of 0.001–0.003 for the present study, which indicates that there is no further MOS left in the design and the structure is optimized to full potential.
(i)The algorithm is tested for its consistency and the solutions are found to reach near global-optima for maximum number of cases.

Appendix A. Supplementary data

Supplementary data associated with this article can be found, in the online version, athttps://doi.org/10.1016/j.compstruct.2018.09.004.

References

[1] Shrivastava S, Mohite PM. Design and optimization of a composite canard control surface of an advanced fighter aircraft under static loading. Curved Layered Struct 2015;2(1):91–105. https://doi.org/10.1515/cls-2015-0006.
[2] Lee D, Morillo C, Oller S, Bugeda G, Onate E. Robust design optimisation of advance hybrid (fiber metal) composite structures. Compos Struct 2013;99:181–92. https://doi.org/10.1016/j.compstruct.2012.11.033.
[3] Kalantari M, Dong C, Davies I. Multi-objective robust optimisation of unidirectional carbon/glass fibre reinforced hybrid composites under flexural loading. Compos Struct 2016;138:264–75. https://doi.org/10.1016/j.compstruct.2015.11.034.
[4] Blasques J, Stolpe M. Maximum stiffness and minimum weight optimization of laminated composite beams using continuous fiber angles. Struct Multidisc Optim 2011;43:573–88. https://doi.org/10.1007/s00158-010-0592-9.
[5] Shrivastava S, Mohite PM, Yadav T, Malagaudanvar A. Multi-objective multi-laminate design and optimization of a carbon fibre composite wing torsion box using evolutionary algorithm. Compos Struct 2018;185:132–47. https://doi.org/10.1016/j.compstruct.2017.10.041.
[6] Weigang A, Dianyu C, Peng J. A single-level composite structure optimization method based on a blending tapered model. Chinese J Aeronaut 2013;26(4):943–7.
[7] Irisarri F, Lasseigne A, Lerroy F, Riche R. Optimal design of laminated composite structures with ply drops using stacking sequence tables. Compos Struct 2014;107:559–69.
[8] Mukherjee A, Varughese B. Design guidelines for ply drop-off in laminated composite structures. Compos Part B: Eng 2001;32(2):153–64. https://doi.org/10.1016/S1359-8368(00)00038-X.
[9] Liu D, Torpov VV, Querin OM, Barton DC. Bilevel optimization of blended composite wing panels. J Aircraft 2011;48:107–18.
[10] Kristinsdottir B, Zabinsky Z, Tuttle M, Neogi S. Optimal design of large composite panels with varying loads. Compos Struct 2001;51:93–102.
[11] Jin P, Zhong X, Yang J, Sun Z. Blending design of composite panels with lamination parameters. Aeronaut J 2016;120(1233):1710–25.
[12] Adams DB, Watson LT, Gürdal Z. Optimization and blending of composite laminates using genetic algorithms with migration. Mech Adv Mater Struct 2003;10(3):183–203.
[13] Seresta O, Gürdal Z, Adams DB, Watson LT. Optimal design of composite wing structures with blended laminates. Compos Part B: Eng 2007;38(4):469–80.
[14] Daoust J, Hoa SV. Parameters affecting interlaminar stresses in tapered laminates under static loading conditions. Polymer Compos 1989;10(5):374–88. https://doi.org/10.1002/pc.750100515.
[15] Zabihollah A, Ganesan R. Buckling analysis of tapered composite beams using a higher order finite element formulation. Polymer Compos 2010;29(17):2663–83. https://doi.org/10.1177/0731684409352124.
[16] Ganesan R, Liu DY. Progressive failure and post-buckling response of tapered composite plates under uni-axial compression. Compos Struct 2008;82(2):159–76. https://doi.org/10.1016/j.compstruct.2006.12.014.
[17] Tsai S, Wu E. A general theory of strength for anisotropic materials. Compos Mater 1971;5(1):58–80. https://doi.org/10.1177/002199837100500106.
[18] Herakovich C. Mechanics of fibrous composites. New Jersey, US: John Wiley & Sons9780471106364; 1997.
[19] Shrivastava S, Mohite PM. Redesigning of a canard control surface of an advanced fighter aircraft: effect of buckling and aerodynamic behavior. Curved Layred Struct 2015;2(1). https://doi.org/10.1515/cls-2015-0010.
[20] Srinivas N, Deb K. Multiobjective optimization using nondominated sorting in genetic algorithms. Evol Comput 1994;2(3):221–48. https://doi.org/10.1162/evco.1994.2.3.221.
[21] Ball N, Sargent P, Ige D. Genetic algorithm representations for laminate layups. Artificial Intelligence Eng 1993;8(2):99–108. https://doi.org/10.1016/0954-1810(93)90020-G.
[22] Jubril A. A nonlinear weight selection in weighted sum for convex multi-objective optimization. Ser Math Inform 2012;27(3):357–72.
[23] Yefim G, Peter D. Sukhoi Su27 Flanker. Specialty Press Publishers and Wholesalers; 2006. [Incorporated].
[24] Howe D. Aircraft conceptual design synthesis. Aerospace series. United Kingdom: Professional Engineering Publishing9781860583018; 2000.
[25] Daley B.N., Lord D.R. Aerodynamic charateristics of several 6 percent thick airfoils at angles of attack from at high subsonic speeds. NACA; 1955.
[26] Schrenck O. NACA Technical Memorandum No. 948. NACA; 1940.
[27] Koerber H, Camanho P. High strain rate characterisation of unidirectional carbon epoxy im7-8552 in longitudinal compression. Compos Part A: Appl Sci Manuf 2011;42(5):462–70. https://doi.org/10.1016/j.compositesa.2011.01.002.
[28] ABAQUS/Standard User's Manual, Version 6.11. Simulia; 2011.
[29] Miettinen K. A Posteriori Methods. In: Nonlinear Multiobjective Optimization. Boston, MA: Springer; 1998. ISBN 978-1-4613-7544-9. doi: 10.1007/978-1-4615-5563-6.